Journal of Experimental and Theoretical Physics, Vol. 91, No. 3, 2000, pp. 515–523.
Translated from Zhurnal Éksperimental’noĭ i Teoreticheskoĭ Fiziki, Vol. 118, No. 3, 2000, pp. 592–601.
Original Russian Text Copyright © 2000 by Zubova, Balabaev, Manevich, Tsygurov.

SOLIDS
Structure

Dynamics of Twist Point Defects with Stretching in a Polymer Crystal

E. A. Zubova[a], *, N. K. Balabaev[b], L. I. Manevich[a], and A. A. Tsygurov[a]
[a]*Semenov Institute of Chemical Physics, Russian Academy of Sciences, Moscow, 117977 Russia*
[b]*Institute of Mathematical Problems of Biology, Russian Academy of Sciences,*
Pushchino, Moscow oblast, 142292 Russia
**e-mail: zubova@center.chph.ras.ru*

Received January 27, 2000

Abstract—A molecular-dynamics simulation of the behavior of a twist point defect with stretching in a chain of an equilibrium polymer crystal (“united” atoms approximation for polyethylene) is performed for immobile and mobile neighboring chains. It is shown that such a defect in a cold polymer crystal possesses soliton-type mobility. The upper limit of the spectrum of soliton velocities is found, and it is the same for both cases. The maximum possible velocity of defects is three times lower than the theoretical limit of the spectrum (which is equal to the velocity of “torsional” sound in an isolated chain). An explanation of the reason for this discrepancy is proposed: because of the interaction of two “degrees of freedom” of the defect (twisting and stretching) the energy of a nonlinear wave is dissipated in the linear modes of the system, which results in effective friction whose magnitude depends strongly on the velocity of the defect. The “boundary of the spectrum of soliton velocities” determines the transition between regimes of strong and weak braking of defects. *© 2000 MAIK “Nauka/Interperiodica”.*

1. INTRODUCTION

To predict the relaxation, plastic, and strength properties as well as the melting temperature of crystals it is necessary to study localized mobile defects—deviations from an ideal structure. Point structural defects (vacancies or inclusions) are responsible for the relaxation properties of solids. The impossibility of directed motion of such defects is the reason why relaxation processes are slow in low-molecular crystals. On account of the strong anisotropy of the properties of polymer crystals (the atoms in a polymer chain are bound with one another by chemical covalent bonds, and the intermolecular interaction is due to weak van-der-Waals forces) vacancies with breaking of intrachain covalent bonds are virtually immobile. However, such crystals can contain different, specifically polymer, point defects, which are due to not the breaking of intrachain bonds but rather the deformation of a chain localized on a small section of the chain.

The concepts of such defects appeared in the physics of polymer crystals after the discovery of the anomalously rapid dielectric relaxation of oxidized polyethylene (see the review in [1]). Analysis of a number of possible molecular mechanisms of this process (see the review in [2]) made it possible to identify as the most likely mechanism the propagation of regions of twisting (by 180°) with stretching (by a half-period of the chain) that have a length of several tens of periods, in the absence of conformational changes, along the chains. It turned out [3, 4] that such defects are also created in the process of premelting of a crystal (their energy is much lower than the energy of purely stretching defects—vacancies of one unit of the chain without twisting).

The quasi-one-dimensional approximation with immobile neighboring chains (see, for example, [5] and the literature cited there) makes it possible to describe a point defect as a soliton-type topological excitation [6]—a localized nonlinear wave propagating with constant subsonic velocity along the chain, changing the state of the chain after it passes and therefore capable of causing rapid relaxation in the crystal.

An approximate analytical description of static point defects in polyethylene was proposed in [7], and a numerical investigation by molecular-mechanics methods was conducted in [8]. However, these works did not consider the question of the mobility of defects and correspondingly the role of defects in the relaxation of a crystal.

The problem of point defects in a polyethylene chain surrounded by immobile neighboring chains has recently been solved by a numerical-variational method [9, 4] (in the “united” atoms model, in which CH_2 groups are replaced by point particles). It was found that in this case point defects possess soliton-type mobility, and the upper limits of the velocity spectrum for different types of defects were calculated.

But, in a more previous work [10] a molecular-dynamics investigation of the behavior of torsional point defects with stretching in a polyethylene crystal was performed in the same “united-atoms” model but

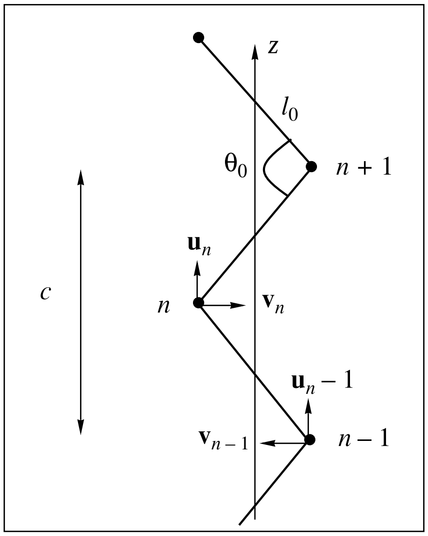

Fig. 1. Model of a polymer crystal (polyethylene with united atoms): parameters of the chain and the local coordinates of the atoms.

with mobile molecules of the first coordination sphere, and it was concluded from the results of the numerical experiment that the mobility of such defects is of nonsoliton type: they stopped rapidly.

However, the arrangement of this experiment was such that defects could stop rapidly for several reasons. In the first place, it was discovered in [11] that purely stretching defects in an equilibrium crystal configuration with all mobile chains in the crystal retain the initial velocities right up to values of the order of 0.6 times the velocity of sound, and for high velocities they slow down to this velocity but do not stop. In nonequilibrium or unstable structures (including the orthorhombic structure, which is nonequilibrium in the "united atoms" model of polyethylene used in [10]), requiring that the chains rotate in order for relaxation to occur, the vacancies stop rapidly. The clearly soliton character of the dynamics of pure vacancies led us to conjecture that the stopping of a defect in [10] was due precisely to the nonequilibrium nature of the initial crystal.

But, in addition, we saw in [11] that friction against the phonon modes of mobile neighboring chains substantially decreased the upper limit of the velocity spectrum even for pure vacancies (from the velocity of sound *c* (theoretical limit) down to ≈0.6 times this value). The interaction of a twist point defect with stretching with the same phonon modes can be much stronger and can even make the soliton mechanism of defect mobility impossible.

The purpose of the present work is to study the dynamics of twist point structural defects with stretching in a polymer crystal with all mobile chains on the basis of the same molecular-dynamics model as the one used in [11].

Our numerical model of a crystal for studying the dynamics of point defects is described in Section 2. An approximate analytical description of the defects is presented in Section 3 for immobile neighboring chains. The results of a molecular-dynamics simulation of the dynamics of defects with immobile and mobile neighboring chains are presented in Section 4. Finally, Section 5 is devoted to a discussion of these results and the conclusions.

2. NUMERICAL MODEL OF A POLYMER CRYSTAL (POLYETHYLENE WITH "UNITED" ATOMS); EQUILIBRIUM CRYSTAL CONFIGURATION

We adopted the following model of a polymer crystal [12] (polyethylene with united atoms; see Fig. 1): the chains are a planar trans-zigzags; the bonds between the atoms (point particles with mass m) are absolutely rigid and their length is l_0; the deformation energies of the valence (θ_n) and conformational (τ_n) angles are

$$U_3(\theta_n) = \frac{1}{2}K_\theta(\theta_n - \theta_0)^2, \qquad (1)$$

$$U_4(\tau_n) = \alpha + \beta\cos\tau_n + \gamma\cos 3\tau_n, \qquad (2)$$

the atoms separated by more than 2 neighbors or belonging to different chains interact according to the law

$$U(r) = \begin{cases} U_{LJ}(r) - U_{LJ}(R), & r \le R \\ 0, & r > R, \end{cases}$$

where $U_{LJ}(r) = 4\epsilon[(\sigma/r)^{12} - (\sigma/r)^6]$ is the Lennard–Jones potential with a minimum at the point $r_0 = 2^{1/6}\sigma$. The numerical values used for the constants are given in Table 1.

Table 1. Parameters of the model crystal

Parameter	Quantity	References	Parameter	Quantity	References
m	14 amu	–	β	1.675 kJ/mole	[13]
l_0	1.53 Å	[13]	γ	6.695 kJ/mole	[13]
θ_0	113°	[13]	ϵ	0.4937 kJ/mole	[14]
K_θ	331.37 kJ/mole	[13]	σ	3.8 Å	[14]
α	8.370 kJ/mole	[13]	R	$2r_0$	–

For the model of the crystal we adopted periodic boundary conditions in all three directions. A rectangular parallelepiped was chosen for the working cell. The leap-frog algorithm [15], taking account of the restrictions imposed by the rigid bonds [16], was used to solve the corresponding classical Lagrangian equations of the first kind numerically. Periodic boundary conditions along the axis of the molecules make it possible to follow the dynamics of a defect for an unbounded time and those in the transverse section of the crystal, to avoid introducing in the transverse section unphysical boundary conditions with a rigidly fixed second coordination sphere. To prevent a soliton from affecting itself the number of molecules in the working cell was chosen so that the image of each molecule was located no closer than in its fourth coordination sphere and the length of the molecule—for a defect of the order of 35 chain periods c long—was assumed to be $200c$ (one period contains two CH_2 groups).

Since the length of the projection of a molecule on its transverse section is $l_\perp = 0.843$ Å and the van-der-Waals radii of the united atoms r_0 are 4.265 Å $\approx 5l_\perp$, the packing of the zigzag planes in the crystal will be close to that of cylinders. Theoretically, two different mechanically equilibrium configurations are possible (see Fig. 2). Both possess a monoclinic cell and close energies. However, the second one is unstable and separates into two domains, each of which corresponds to the first configuration [11], as a result of relaxation. The parameters of a stable equilibrium structure a and b depend on the cutoff radius R. Table 2 presents data on the relaxation of samples for different values of R. The period along the axis of a molecule is always $c = 2.554$ Å. The density of the sample is $\rho = 1.155$ g/cm^3.

Molecular-dynamics simulation of a polyethylene crystal in the united-atoms model has shown [11] that the potential energy does not have a local minimum for an orthorhombic structure for any value of the cell parameters. The numerical experiment reveals the appearance of this minimum only in a model of polyethylene in which the CH_2 group is represented by three spatially separated force centers. Thus, the possibility of the existence of an orthorhombic structure in polyethylene is due to the presence of side groups and not the form of the backbone of the chains.

3. APPROXIMATE ANALYTICAL DESCRIPTION OF A TWIST POINT DEFECT WITH STRETCHING IN A CHAIN OF A POLYMER CRYSTAL

We shall consider the simplest description of the dynamics of a twist defect with stretching in the chain of a polymer crystal in the immobile-neighbors approximation using the continuum model.

The effective substrate potential generated for the nth atom by immobile neighbors in a stable equilibrium monoclinic lattice of a polymer crystal in the “united” atoms model should have two wells with different minima at the points (ϕ_n, ψ_n): $(0, 0)$ and (π, π). Here ϕ_n is the angle in a cylindrical coordinate system whose axis is directed along the axis of a molecule, $\psi_n = (2\pi/c)u_n$ (u_n is the longitudinal displacement from the position of equilibrium).

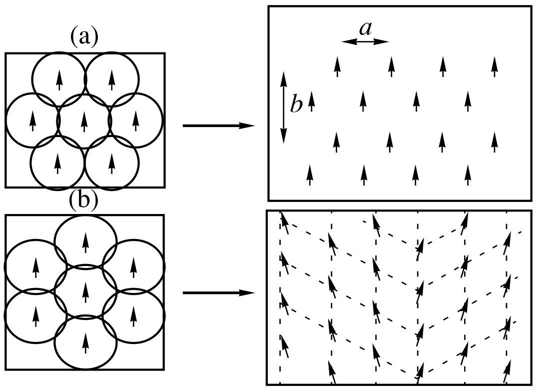

Fig. 2. Possible equilibrium configurations for planar zigzag packing: (a) stable, (b) unstable (the period of the transverse section of the molecules is shown; the arrows show the direction from the nearest atom of the molecule under the plane to the nearest above the plane).

Numerically, the substrate potentials obtained by calculating the energy of the crystal with all molecules secured except one, which can move and rotate (as a whole) along the axis. In the stable equilibrium configuration of the crystal the function

$$V(\phi_n, \psi_n) = A(1-\cos\phi_n\cos\psi_n) + B(1-\cos 2\phi_n) \quad (3)$$

with $A \approx 0.274$ kJ/mole and $B \approx 0.865$ kJ/mole approximates the substrate potential with an error of less than 10% of its maximum value. The level lines of the function (3) are shown in Fig. 3.

Adding a term $C(1-\cos 4\phi_n)$ with $C = -0.067$ kJ/mole to the potential (3) decreases the error to 2%. We shall discuss in Section 5, after presenting the results of the molecular-dynamics simulation, how this addition can influence the dynamics of a defect.

In our analysis we neglect the dependence of the potential V on the third coordinate—transverse displacements v_n, since for long-wavelength waves (with characteristic scale much greater than the distance between the atoms of a chain) the transverse displacements of the atoms are much smaller than the longitudinal displacements (see Appendix A). The consequences (except for a small change in the form of the analytical solution) of taking account of the depen-

Table 2. The parameters a and b (in Å) of the equilibrium crystalline configuration for different cutoff radii R

Parameter	$R = 1.8r_0$	$R = 2r_0$
a	3.998	3.980
b	7.994	7.966

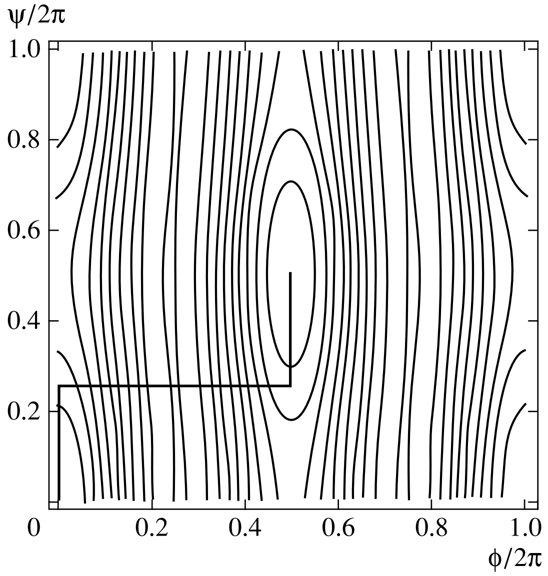

Fig. 3. Level lines of the potential surface (3) for a substrate, generated by immobile neighboring chains, in the (ϕ, ψ) plane. The broken line shows the "orbit" of the zeroth analytical approximation ($L_\phi/L_\psi \longrightarrow 0$) in the solution of the system of equations (8).

dence of the potential on this coordinate will be discussed in Section 5. Here we shall confine our attention to the main interaction of the two basic degrees of freedom of an atom.

The rigid-bond condition determines the relation between the longitudinal and transverse displacements u and v of the atoms (see Fig. 1). Switching to the continuum approximation (which is justified because of the relative weakness of the intermolecular interaction) and neglecting dispersion and nonlinearity, which are due to intramolecular interactions (see [17] for a more accurate continuum description), we obtain the Lagrangian system

$$L = \int \frac{dx}{l_0 s_0}\left[I_\phi \frac{\phi_t^2}{2} + I_\psi \frac{\psi_t^2}{2} - K_\phi \frac{\phi_x^2}{2} - K_\psi \frac{\psi_x^2}{2} - V(\phi, \psi)\right], \quad (4)$$

where the constants are related with the parameters of the numerical model of the crystal by the relations (see Appendix B)

$$I_\phi = m\left(\frac{l_0 c_0}{2}\right)^2, \quad I_\psi = m\left(\frac{l_0 s_0}{\pi}\right)^2, \quad (5)$$

$$(s_0 = \sin(\theta_0/2), \quad c_0 = \cos(\theta_0/2));$$

$$K_\phi = l_0^2(\beta + 9\gamma), \quad (6)$$

$$K_\psi = \left(\frac{2 l_0 s_0^2}{\pi c_0}\right)^2 K_\theta. \quad (7)$$

Here I_ϕ, I_ψ and K_ϕ, K_ψ are, respectively, the inertial and stiffness parameters of the chain—"torsional" (with respect to ϕ) and "longitudinal" (with respect to ψ). For our numerical values of the crystal parameters, $I_\phi/I_\psi \approx 1.08$ and $K_\phi/K_\psi \approx 0.29$.

Thus, we have obtained a very simple model for two coupled fields with different "stiffness characteristics" and "inertial properties," and the relation between them is due only to the anharmonicity of the external substrate potential.

The Lagrangian (4) with the potential function (3) corresponds to coupled equations describing the evolution of the fields ϕ and ψ:

$$\begin{aligned} I_\phi \phi_{tt} - K_\phi \phi_{xx} + A\sin\phi\cos\psi + 2B\sin 2\phi &= 0, \\ I_\psi \psi_{tt} - K_\psi \psi_{xx} + A\sin\psi\cos\phi &= 0. \end{aligned} \quad (8)$$

It is easy to see that the variables ϕ and ψ in the linearized equations of the system separate and give two branches of the dispersion curve with two sound velocities: torsional sound $v_\phi = \sqrt{K_\phi/I_\phi} \approx 7.63$ km/s and longitudinal sound $v_\psi = \sqrt{K_\psi/I_\psi} \approx 14.70$ km/s. In the continuum model of a chain without a substrate these are the maximum propagation velocities of small-amplitude disturbances along ϕ and ψ, respectively.

Let us assume that the system of equations (8) possesses a solution in the form of a topological solitary nonlinear wave moving with velocity $v \geq 0$ in a direction of positive values of x, i.e., in the form of "coupled" kinks

$$\phi = \phi(x - vt), \quad \psi = \psi(x - vt),$$

where the functions ϕ and ψ are such that as time t varies from $-\infty$ to $+\infty$ they vary from π to 0. Then this wave corresponds to a kink of twisting by 180° and stretching by a half-period of the chain. When such a wave passes along the chain all particles will move in turn into the position of the nearest neighbor in the direction of negative values of x.

If a solution of this form exists, then the problem consists simply of finding the correct "orbit" in the $\phi\psi$ plane. The exact solution of such a problem is known for identical stiffness and inertial parameters of the fields for a number of simple polynomial potentials $V(\phi, \psi)$ (see [18] and the references cited there, as well as [19]). In our case successive approximations to the solution can be found assuming that the kink width L_ϕ with respect to ϕ is much smaller than the kink width L_ψ with respect to ψ. Indeed, the "torsional" stiffness K_ϕ of the chain is approximately 3.4 times smaller than the longitudinal stiffness K_ψ, and the substrate is stiffer for ϕ than for ψ because of the presence of the large term $B(1 - \cos 2\phi_n)$ in the potential. In the limit $L_\phi/L_\psi \longrightarrow 0$ the orbit will approach the broken line shown in Fig. 3. For a finite value of the parameter the first approximation to the solution can be obtained by assuming that in the equation for ϕ the kink with respect to ψ is "infinitely wide" and setting $\psi \longrightarrow \pi/2$. The equation for ψ can be solved in two regions: for $x - vt < 0$, replacing ϕ by 0, and for $x - vt \geq 0$, making the substitution $\phi \longrightarrow \pi$ and matching the solutions at the point $x - vt = 0$ (this method of solving a similar system of equations was proposed in [5]). In our case all three equations reduce to the sine-Gordon equations. After matching the solutions we obtain

$$\phi_1 = 2\arctan\exp\left(\frac{x - vt}{L_\phi\sqrt{1-(v/v_\phi)^2}}\right),$$
$$L_\phi = \sqrt{\frac{K_\phi}{4B}} \approx 5.08\frac{c}{2}; \tag{9}$$

$$\psi_1 = \begin{cases} 4\arctan\exp\left(\dfrac{x - vt}{L_\psi\sqrt{1-(v/v_\psi)^2}} - \ln\tan\left(\dfrac{3\pi}{8}\right)\right), \\ x - vt < 0 \\ 4\arctan\exp\left(\dfrac{x - vt}{L_\psi\sqrt{1-(v/v_\psi)^2}} + \ln\tan\left(\dfrac{3\pi}{8}\right)\right) - \pi, \\ x - vt \ge 0, \end{cases} \tag{10}$$
$$L_\psi = \sqrt{\frac{K_\psi}{A}} \approx 33.5\frac{c}{2},$$

and the kink velocity v must be less than the lowest of the velocities v_ϕ and v_ψ. We can see that the parameter $L_\phi/L_\psi \approx 0.152$ is indeed small.

When the term $C(1 - \cos 4\phi_n)$ is included in the potential the form of the kink with respect to ϕ will be the solution not of a simple but rather a double sine-Gordon equation.

In what follows we shall seek the solution in the form $\phi = \phi_1 + \phi_2 + \ldots$ $\psi = \psi_1 + \psi_2 + \ldots$, refining the form of the kinks. However, it is important to note that this procedure, even though it leads to the dependence of the form of the kink with respect to ϕ on the parameters L_ψ and v_ψ and the form of the kink with respect to ψ on the parameters L_ϕ and v_ϕ, it cannot change the maximum velocity of a kink. In the opposite approximation (the case of identical stiffness and inertial parameters of the field [19]) the exact solution also admits arbitrary subsonic velocities of coupled waves.

Thus, if the interaction $V(\phi, \psi)$ is such that there exists an "orbital" solution in the form of a coupled solitary wave $\phi - \psi$, then for the potential (3) with a small value of the parameter L_ϕ/L_ψ the form of this wave is given approximately by Eqs. (9) and (10) and the velocity $v < v_\phi < v_\psi$.

In summary, a twist defect with stretching (no breaking of covalent bonds (Fig. 4)) can move along the chain with subsonic velocity $v < v_\phi < v_\psi$, maintaining localization and not disrupting the crystal structure outside the region of the defect. This means that for velocities that are not too close to the sound velocity the dynamics of defects should be of a soliton character (as $v \longrightarrow v_\phi$ the discreteness and the intramolecular nonlinearity can no longer be neglected, since the solitons are too "narrow").

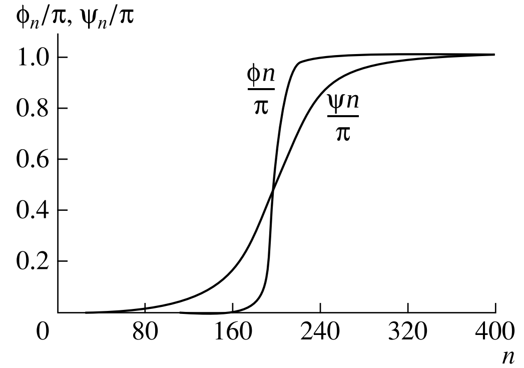

Fig. 4. Static twist point defect with stretching in a chain in a polymer crystal: the coordinates of the atoms in a chain with a defect in a cylindrical coordinate system with the axis directed along the axis of the molecule (see Fig. 1): the steeper curve is for the angle ϕ_n/π (ϕ in radians), the more gently sloping curve is for $\psi_n/\pi = (2/c)u_n$ (u_n is the longitudinal displacement from the position of equilibrium); the form of the defect after relaxation of the crystal in 15 ps is shown, and the difference of the curves shown from the analytical solution (9) and (10) does not exceed 0.005.

4. RESULTS OF MOLECULAR-DYNAMICS SIMULATION OF THE BEHAVIOR OF TWIST DEFECTS WITH STRETCHING IN A POLYMER CRYSTAL

The following time scales are characteristic for the system under study: the travel time of longitudinal sound over one period of the chain is approximately 1.7×10^{-2} ps, the width of a defect along ψ is about 0.58 ps, the travel time of "torsional" sound over the width of a defect along the ϕ coordinate is approximately 0.17 ps.

In the molecular-dynamics experiment, for one of the molecules of a crystal, which has relaxed and cooled down to 0.01 K, we set the atomic displacements and velocities according to the approximate analytic formulas (9) and (10) and observed the evolution of a defect for a prolonged time (of the order of hundreds of picoseconds).

Our analytical approximation (9) and (10) seems to be very rough: kinks "are not coupled." But it turns out that for a static kink the approximation fits the experimentally observed curves (Fig. 4) with an error of less than 0.5% of the magnitude of the jump.

In the numerical experiment we followed the position x_{cm} and velocity v_{cm} of the center of mass of a chain with a defect, which were easily converted to the displacement and velocity of a defect: $x_{\mathrm{def}} = -N_1[x_{\mathrm{cm}} - x_{\mathrm{cm}}(t = 0)]$ and $v_{\mathrm{def}} = -N_1 v_{\mathrm{cm}}$ ($N_1 = 399$ is the number of atoms

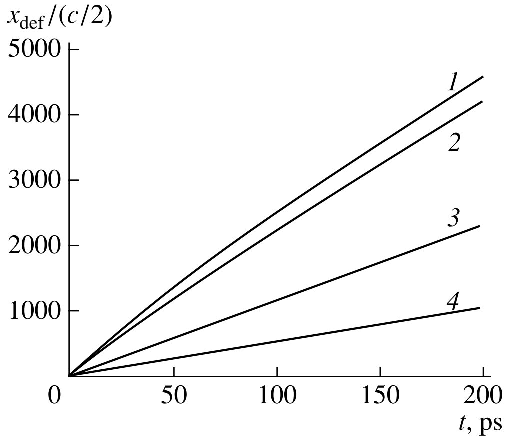

Fig. 5. Dynamics of defects in a chain on a substrate generated by stationary neighboring chains: displacement of defects (in half-periods of the chain) with velocities (*1*) 0.9, (*2*) 0.45, (*3*) 0.2, and (*4*) 0.1 of the velocity of the lower (torsional) sound as a function of time.

in a chain with a defect). With this conversion, because of the thermal vibrations of the atoms (for sample temperature of the order of several Kelvins) high-frequency oscillations are superposed on the true value of the velocity of a defect. These oscillations have no relation to the velocity, and we filtered them out to make the picture clearer.

4.1. Dynamics of Twist Defects with Stretching in a Chain on a Substrate, Generated by Stationary Neighboring Chains

We shall now describe the results of a simulation of the evolution of twist defects with stretching with initial velocities of approximately 0.9, 0.45, 0.2, and 0.1 times the velocity of the lower (torsional) sound (6.875, 3.437, 1.514, and 0.757 km/s) in a crystal in stable equilibrium (Fig. 2a) with clamped neighboring molecules.

As expected, soliton-type mobility of defects is clearly observed in the numerical experiment (see Fig. 5): they move along the chain with constant average velocity, traversing in 200 ps 4378, 4003, 2194, and 937 CH_2 groups (half-periods of the chain), respectively. By analogy with the dynamics of pure vacancies, one would expect that the defects would retain their initial velocities. However (Figs. 6 and 7), only two of the slowest defects retain their velocities. The velocity of fast defects decreases in the first 7 ps to 0.43 (from 0.9) and 0.39 (from 0.45) from the velocity of sound, and in the next 193 ps it slowly decreases to 0.34 and 0.33, respectively.

This picture strongly resembles the evolution of pure vacancies in the presence of mobile neighboring chains [11], when the energy of high-velocity vacancies was transferred to neighboring chains because of the stronger interaction, and the intensity of the interaction with phonon modes of the surrounding molecules decreased sharply with decreasing velocity of the vacancy, so that the (first) limit of the velocity spectrum of purely stretching solitons (approximately 0.6 times the upper (longitudinal) sound) in the presence of mobile neighboring chains arose.

For the propagation of a twist defect with stretching, the energy of a nonlinear wave in the coordinate ψ is transferred into phonon modes ϕ (or, possibly, other modes; see the discussion in Section 5) because of the interaction of the fields ϕ and ψ. Conversely, the energy of the nonlinear wave in the coordinate ϕ is transferred

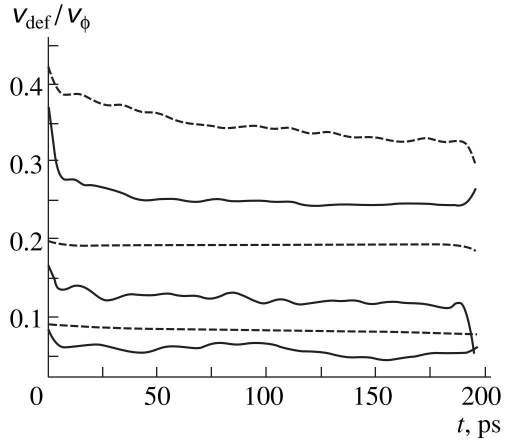

Fig. 6. Dynamics of defects in a polymer crystal: variation of the average velocity of defects with time with immobile (dashed lines) and mobile (solid lines) neighboring chains; the initial velocities of the defects are 0.45, 0.2, and 0.1 times the velocity of lower (torsional) sound (the sharp cutoffs at the end of the plots are not a physical effect; they are due to the averaging procedure).

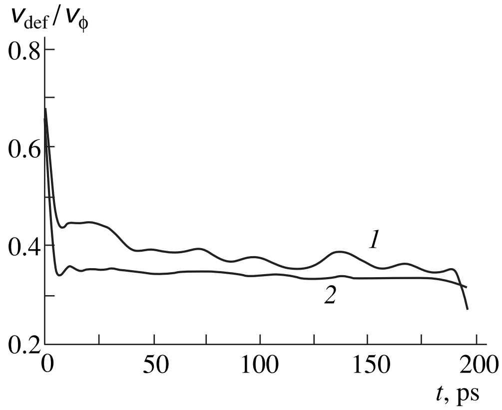

Fig. 7. Dynamics of a defect with initial velocity 0.9 times the velocity of lower (torsional) sound in a polymer crystal: variation of the average velocity with time with (*1*) immobile and (*2*) mobile neighboring chains (the sharp cutoffs at the end of the plots are not a physical effect; they are due to the averaging procedure).

into phonon (or other) modes ψ. The intensity of this interaction, just as the interaction of a purely stretching soliton with the phonon modes of neighboring mobile chains, decreases sharply with decreasing velocity of the wave, and the (second) limit of the velocity spectrum of twist solitons with stretching (~0.34 times the lower (torsional) sound) arises even with immobile neighboring chains. For initial defect velocities much higher than this limit the defect slows down (with large oscillations of even the average velocity; see Fig. 7, curve *1*). These oscillations are still noticeable with the initial velocity of the defect 0.45 times the "torsional" sound (above the limit where the velocity decreases; see Fig. 6, upper curve), but they are no longer noticeable for slow defects, whose initial velocities are remain unchanged.

4.2. Dynamics of Torsional Defects with Stretching in a Chain Surrounded by Mobile Neighboring Chains

The simulation results for the evolution of torsional defects with stretching with initial velocities of the order of 0.9, 0.45, 0.2, and 0.1 times the velocity of lower (torsional) sound in a crystal in stable equilibrium (Fig. 2a) with all mobile molecules are very close to the results obtained for a sample in which the neighboring chains are clamped.

Soliton-type mobility of defects is observed in the numerical experiment: they move steadily along the chain; the corresponding plot is very similar to Fig. 5, the only difference being that the tangents of the slope angles of the curves are smaller (see Figs. 6 and 7 for the velocities) and the average velocities fluctuate somewhat and decrease slightly even for the two slowest defects.

Deformations (along the axis of the molecule and along the angle) accompanying a defect during motion along a chain ("shadows") arise on the mobile neighboring chains near a defect. The form of the "shadows" can be determined analytically in perturbation theory for a purely stretching defect [20]. In the numerical experiment we took as the initial condition the atomic displacements and velocities using the analytical formulas (9) and (10) only on a chain with a defect. It is probably because the initial conditions are not completely "correct" that the velocities of the defects in the steady state with mobile neighbors turned out to be less than for immobile neighbors.

The oscillations of the magnitude and the hardly noticeable additional decrease of the velocities (Fig. 6) are the only direct consequences of the mobility of the neighboring chains in the crystal. It is obvious why this effect is so weak: the velocities of the defects are low, and the interaction of the defects with the phonon modes of neighboring chains become substantial, as we saw in [11], only for velocities higher than the first limit $\sim 0.6 v_\psi \approx 1.2 v_\phi$. It is interesting that near this first boundary (with initial defect velocity $0.9 v_\phi$) friction on the phonon modes of neighboring mobile chains is still so large that the velocity of a defect decreases much more rapidly than for stationary neighboring chains, and it decreases immediately down to the value of the lower second boundary, after which it stops decreasing and no longer fluctuates (Fig. 7, curve *2*).

5. DISCUSSION

In the present paper it was found by molecular-dynamics simulation that the dynamics of twist point defects with stretching in a (cold) polymer crystal is of a soliton character: defects retain their initial velocities if they lie below a certain value (~0.34 times the velocity of the lower (torsional) sound—the theoretical limit of the spectrum). The motion of a twist defect with stretching in a chain in a polymer crystal with velocities below torsional sound is essentially independent of whether the surrounding chains are mobile or immobile.

In [21] the upper limit of the velocity spectrum of twist solitons with stretching remained unnoticed in the molecular-dynamics study of defects in a close model of polyethylene with united atoms because the evolution of the solitons was followed for only a short time (in the time available the solitons could traverse only several tens of CH_2 groups). In [4, 9] it was found for other values of the parameters of the model crystal (with immobile neighboring chains) by a numerical-variational method (it was found that a numerical extremum of the Lagrangian of the system exists for solutions in the form of a solitary wave only for velocities below a certain limit), but the reason why this limit appeared was not discussed.

We believe that the reason is as follows: because the fields ϕ and ψ interact with one another energy is transferred from the nonlinear wave in the coordinate ψ into phonon modes ϕ (or modes localized near a kink) and, conversely, energy is transferred from the nonlinear wave in the coordinate ϕ into phonon modes ψ (or modes localized near a kink).

We note that, of course, for the sine-Gordon equation no localized linear modes other than a translational mode exist. However, in our analytical approximation we actually "separated" the kinks, and only because of this our equations all reduce to the sine-Gordon equations. In addition, in our theoretical analysis we confined our attention to the simplest potential for the interaction of the fields (3), which, however, approximates a real substrate to within about 10%. To increase the accuracy to 2%, a term $C(1 - \cos 4\phi_n)$ with $C = -0.067$ kJ/mole must be added; this leads to a double sine-Gordon equation in the variable ϕ. Finally, multiple harmonics can effectively be added to the main term in (3) when the transverse displacements of atoms in the zigzag plane are taken into account.

For the perturbed sine-Gordon equation, however, it is known that, just as in the nonintegrable φ^4 model, the energy of the directed motion of a defect can be transferred not only to phonon but also to localized modes, which can be excited "around" a nonlinear wave (for certain types of perturbations see [22]; for the double sine-Gordon equation the form of these modes was obtained in [23]).

Thus, because the energy of a nonlinear wave is dissipated into linear modes of the system an effective friction arises, and the magnitude of this friction decreases sharply with decreasing velocity of the wave, so that a limit of the velocity spectrum of a twist soliton with stretching appears even with stationary neighboring chains. The friction against the phonon modes of neighboring mobile chains [11] is much smaller than the interaction of the torsional and longitudinal degrees of freedom of a defect, and consequently it is this interaction that limits the velocity of a defect in a cold polymer crystal.

Of course, the "orbital" analytical approximation in Section 3 cannot describe such a transfer of energy from a nonlinear wave into linear modes of the system. Further study of the evolution of the interacting fields is required (analytical "nonorbital" and numerical).

ACKNOWLEDGMENTS

This work was supported by the Russian Foundation for Basic Research (project no. 98-03-33366) and the Commission on Work with Young People of the Russian Academy of Sciences.

APPENDIX A

Possibility of Ruling Out Transverse Displacements of Atoms of a Flat Trans-Zigzag for Long Wavelengths in a Model with Absolutely Rigid Bonds between Atoms

The condition for the interatomic bonds to be rigid gives in the linear approximation

$$c_0(v_{n+1} + v_n) \approx s_0(u_{n+1} - u_n), \qquad \text{(A.1)}$$

where u_n and v_n are the local Cartesian coordinates of the atoms (see Fig. 1), and the third coordinate w_n forms a triplet with them.

If we confine our attention to waves with long wavelengths and switch from a discrete set $\{u_n(t)\}$ to a field $u(x, t)$ (and similarly for v and w), then Eq. (A.1) becomes

$$v(x, t) \approx \frac{s_0^2}{2c_0} l_0 u_x(x, t).$$

We can see that $v \sim (c/4L)u$ (c is the period of the chain and L is the characteristic scale of variation of u). Thus, for long wavelengths the coordinate v can be neglected in the zeroth approximation.

APPENDIX B

Relation between the Constants of the Analytical Model and the Parameters of the Numerical Model of the Crystal

The inertial constants (5) can be easily obtained by writing the kinetic energy of an atom in cylindrical coordinates (z, r, ϕ) with r = const.

To express the constant K_ψ in terms of K_θ, we shall write the increment to the angle θ_n in the linear approximation:

$$\theta_n - \theta_0 \approx \frac{c_0}{l_0}(u_{n+1} - u_{n-1})$$

$$+ \frac{s_0}{l_0}(v_{n+1} + 2v_n + v_{n-1}).$$

It is independent of w (in the linear approximation). Using Eq. (A.1) it becomes

$$\theta_n - \theta_0 \approx \frac{1}{l_0 c_0}(u_{n+1} - u_{n-1}). \qquad \text{(B.1)}$$

Switching to the variable $\psi_n = (2\pi/c)u_n$, we obtain from the formula (1) for the deformation energy of the valence angle $U_3(\theta_n - \theta_0)$ and the relation (B.1) the expression (7) for K_ψ.

To obtain the constant K_ϕ we note that the conformational angle τ_n between the atomic planes [nth, (n + 1)st, (n +2)nd] and [(n – 1)st, nth, and (n + 1)st] with slow variation (for long-wavelength waves) is $\tau_n = \pi - \chi_n$, $\chi_n \ll 1$. The angle χ_n in the linear approximation does not depend on u_n and v_n and is equal to

$$\chi_n \approx \frac{1}{2l_0 c_0 s_0}(w_{n+2} + w_{n+1} - w_n - w_{n-1}).$$

In a cylindrical coordinate system with r = const this difference can be easily represented in terms of the difference of the angles ϕ_j:

$$\chi_n \approx \frac{1}{4s_0}(\phi_{n+2} + \phi_{n+1} - \phi_n - \phi_{n-1}). \qquad \text{(B.2)}$$

Using the harmonic (in the small angle χ_n) approximation of the potential $U_4(\tau_n)$ of the conformational angle and switching to the continuum approximation, we obtain from Eqs. (2) and (B.2) the relation (6) between K_ϕ and the constants β and γ for the numerical potential.

REFERENCES

1. R. H. Boyd, Polymer **26**, 323 (1985).
2. R. H. Boyd, Polymer **26**, 1123 (1985).
3. L. I. Manevich and A. V. Savin, Vysokomol. Soedin., Ser. A **40**, 931 (1998).
4. A. V. Savin and L. I. Manevitch, Phys. Rev. B **58**, 11386 (1998).

5. V. V. Ginzburg, L. I. Manevich, and N. G. Ryvkina, Mekh. Kompoz. Mater. **2**, 249 (1991).
6. *Solitons in Action*, Ed. by K. Lonngren and A. Scott (Academic, New York, 1978; Mir, Moscow, 1981).
7. V. V. Ginzburg and L. I. Manevich, Fiz. Tverd. Tela (Leningrad) **32**, 2414 (1990) [Sov. Phys. Solid State **32**, 1401 (1990)].
8. D. H. Reneker and J. Mazur, Polymer **29**, 3 (1988).
9. L. I. Manevich and A. V. Savin, Vysokomol. Soedin., Ser. A **40**, 788 (1998).
10. D. W. Noid, B. G. Sumpter, and B. Wunderlich, Macromolecules **24**, 4148 (1991).
11. E. A. Zubova, N. K. Balabaev, and L. I. Manevich, Zh. Éksp. Teor. Fiz. **115**, 1063 (1999) [JETP **88**, 586 (1999)].
12. N. K. Balabaev, O. V. Gendel'man, M. A. Mazo, and L. I. Manevich, Zh. Fiz. Khim. **69**, 24 (1995).
13. D. W. Noid, B. G. Sumpter, and B. Wunderlich, Macromolecules **23**, 664 (1990).
14. D. Rigby and R. J. Roe, Macromolecules **22**, 2259 (1989).
15. M. P. Allen and P. J. Tildesley, *Computer Simulation of Liquids* (Clarendon, Oxford, 1987).
16. P. G. Khalatur, N. K. Balabaev, and A. S. Pavlov, Mol. Phys. **59**, 753 (1986).
17. L. I. Manevitch and A. V. Savin, Phys. Rev. E **55**, 4713 (1997).
18. R. Rajaraman, *Solitons and instantons* (North-Holland, Amsterdam, 1982; Mir, Moscow, 1985).
19. D. Bazeia and E. Ventura, Chem. Phys. Lett. **303**, 341 (1999).
20. E. A. Zubova and L. I. Manevich, in *Proceedings of Scientific Conference of Semenov Institute of Chemical Physics, Russian Academy of Sciences, Moscow, 1999*, p. 46.
21. Fei Zhang and M. A. Collins, Phys. Rev. E **49**, 5804 (1994).
22. O. Braun, Y. Kivshar, and M. Peyrard, Phys. Rev. E **56**, 6050 (1997).
23. P. Sodano, M. El-Batanouny, and C. R. Willis, Phys. Rev. B **34**, 4936 (1986).

Translation was provided by AIP